Electronic Supplementary Material (ESI) for RSC Advances.

[Electronic Supplementary Information]

Characterization and Electrochemical Properties of Iron-doped Tetrahedral Amorphous Carbon (ta-C) Thin Films

Jarkko Etula,*[a] Niklas Wester,[a] Sami Sainio,[a] Tomi Laurila[b] and Jari Koskinen[a]

[a]Department of Chemistry, School of Chemical Technology, Aalto University, P.O. Box 16100, FI-00076 Aalto, Finland.
[b]Department of Electrical Engineering and Automation, School of Electrical Engineering, Aalto University, 02150 Espoo, Finland

Contents

Supplementary A: X-ray reflectivity

This section summarizes additional experimental XRR results on p-FCVA deposition rate calibration series of iron and ta-C used to calculate the deposition rates as moles (mol). Figure S1 shows the XRR results on the deposited calibration samples of iron and carbon (3 of each). Figure S2 shows the calculated deposition rates in thickness, plotted as linear regressions for iron and ta-C. Molar deposition rates can be calculated using the thickness and density parameters tabulated in Tables S1 and S2.

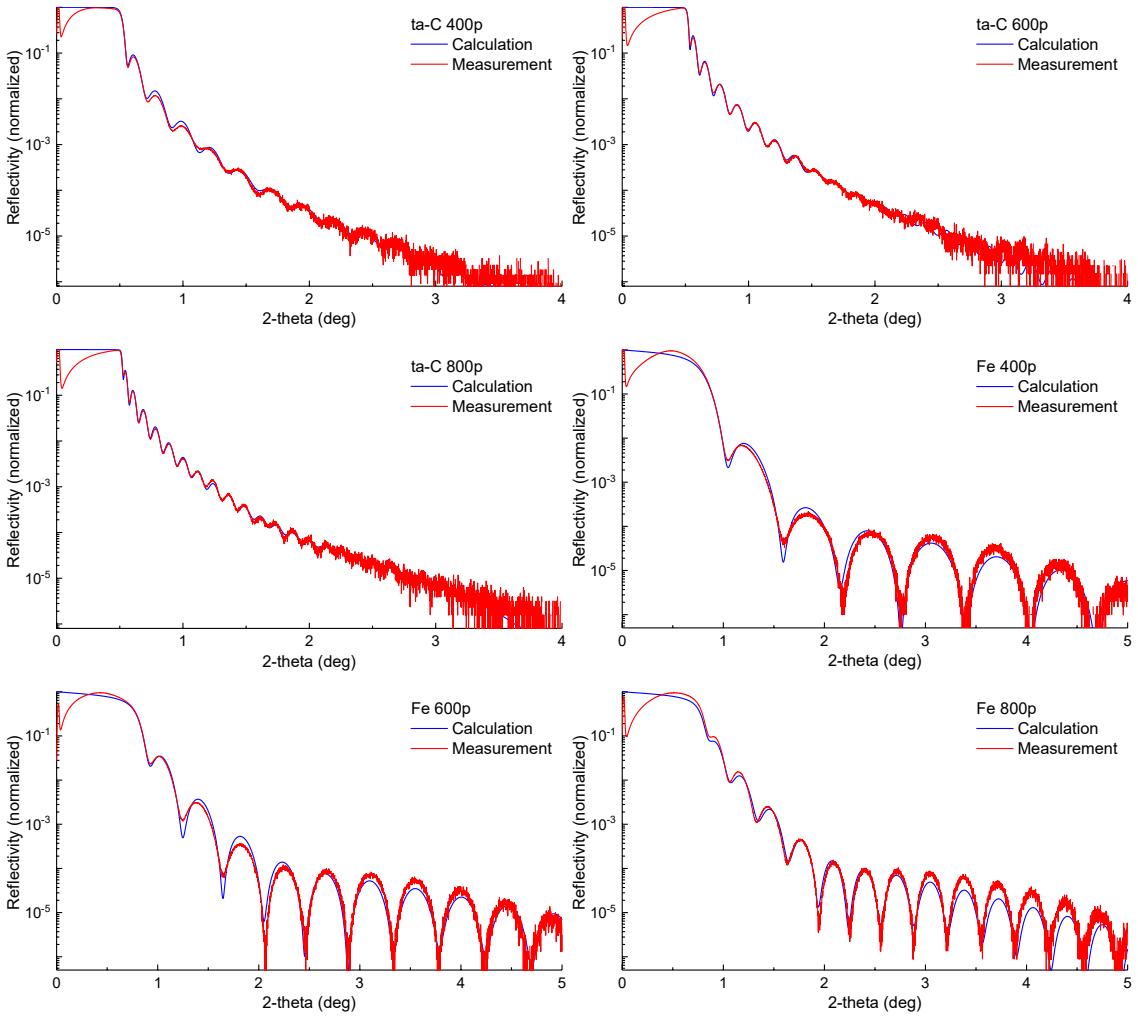

Figure S1. FCVA deposition rate calibration series. X-ray reflectivity scans of ta-C (ta-C 400p, 600p, and 800 pulses) and iron (Fe 400p, 600p, and 800 pulses) showing experimental and simulation data in red and blue, respectively. Tables S1 and S2 show the corresponding XRR layer parameters.

Table S1. X-ray reflectivity results of ta-C calibration samples (ta-C 400p, ta-C 600p, and ta-C 800p) calculated from Figure S1. Complete XRR simulation profiles are shown comprising surface a-C and core ta-C layers: thickness t (nm), density ρ (g/cm^3), roughness R_q (nm). Red values denote fixed parameters.

	ta-C 400p			ta-C 600p			ta-C 800p		
Layer	t	ρ	R_q	t	ρ	R_q	t	ρ	R_q
a-C	1.38	1.92	0.79	1.93	2.26	0.68	2.95	2.76	0.74
ta-C	34.27	2.97	2.47	50.20	3.05	1.30	63.58	3.07	0.10
SiO_2	2.00	2.20	2.01	0.39	2.20	1.43	1.64	2.20	1.81
Si	0.00	2.33	0.81	0.00	2.33	0.00	0.00	2.33	0.96

Table S2. X-ray reflectivity results of iron calibration samples (Fe 400p, Fe 600p, and Fe 800p) calculated from Figure S1. Complete XRR layer profiles are shown of 3 separately simulated iron layers of different properties: thickness t (nm), density ρ (g/cm^3), roughness R_q (nm). Red values denote fixed parameters.

	Fe 400p			Fe 600p			Fe 800p		
Layer	t	ρ	R_q	t	ρ	R_q	t	ρ	R_q
Fe 1	1.24	6.15	1.88	0.04	6.44	1.78	1.88	3.15	0.35
Fe 2	11.31	7.87	0.35	17.18	7.90	0.02	23.25	7.80	1.12
Fe 3	2.02	4.51	1.16	1.87	5.04	0.88	0.30	3.75	2.00
SiO_2	1.10	2.20	0.00	1.00	2.20	0.00	1.40	2.20	0.00
Si	0.00	2.33	0.00	0.00	2.33	0.00	0.00	2.33	0.00

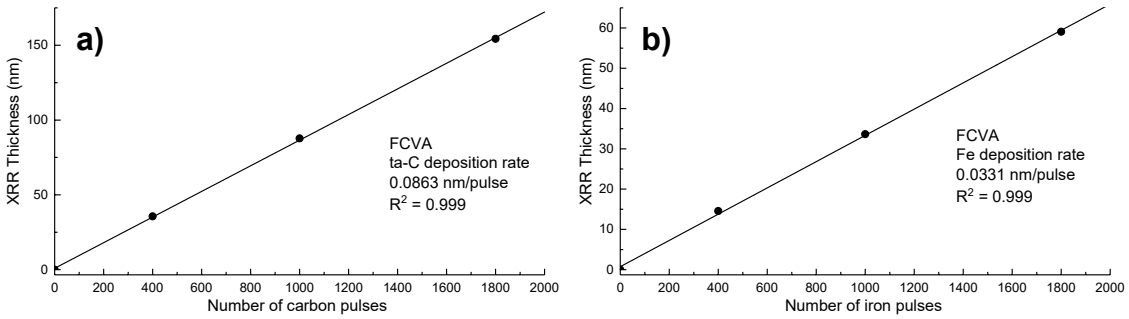

Figure S2. FCVA thickness deposition rates plotted as linear regressions for a) ta-C, and b) iron. Intersection of y-axis is equal to zero.

Table S3 summarizes Tables S1 and S2 to show the relative changes in total film thickness and average density. Since calibration series samples of ta-C include a surface a-C layer, and iron samples consist of multiple Fe layers of different densities, average densities were calculated as a thickness-weighted average.

Table S3. FCVA deposition rate calibration summary ta-C and Fe. Average XRR density is calculated as a thickness-weighted average.

Sample type	Total XRR Thickness (nm)	Average XRR Density (g/cm^3)	Deposition rate (nm/pulse)
ta-C 400p	35.66	2.93	
ta-C 600p	52.13	3.02	0.0863
ta-C 800p	66.53	3.05	
Fe 400p	14.56	7.26	
Fe 600p	19.08	7.62	0.0331
Fe 800p	25.43	7.41	

The full XRR layer profiles for measured Fe/ta-C samples and reference ta-C are exhibited in Table S4. The XRR simulations were single layers of Fe/ta-C with the expected Fe at% used as the atomic composition of the layer simulation. The ta-C reference was simulated without the surface a-C layer.

Table S4. Complete XRR profiles for the primary Fe/ta-C samples in the manuscript. As required by XRR simulations, different layer profiles were developed for each Fe/ta-C layer based on different expected Fe:C atomic compositions. Thickness t (nm), density ρ (g/cm^3), roughness R_q (nm). Red values denote fixed parameters.

Fe/taC sample	2 at% Fe			5 at% Fe			10 at% Fe			ta-C		
Layer	t	ρ	R_q	t	ρ	R_q	t	ρ	R_q	t	ρ	R_q
2 at% Fe:C	32.04	3.10	0.44									
5 at% Fe:C				30.40	3.33	0.58						
10 at% Fe:C							32.53	3.64	0.76			
carbon										35.87	3.04	0.38
SiO_2	0.86	2.20	1.31	0.72	2.20	1.22	1.06	2.20	1.41	1.27	2.20	1.32
Si	0.00	2.33	0.42	0.00	2.33	0.00	0.00	2.33	0.24	0.00	2.33	0.27

Supplementary B: X-ray photoelectron spectroscopy (XPS) wide atomic concentrations and survey spectra

Table S5. Detailed X-ray photoelectron spectroscopy (XPS) wide atomic concentrations (at%) from 3 survey spectra of Fe/ta-C. Charge correction references (Whatman filter paper) are also shown.

Sample	#	C 1s	O 1s	N 1s	Fe 2p	notes
ta-C ref p1	3	95.6 %	4.2 %	0.2 %		
ta-C ref p2	4	95.8 %	3.9 %	0.3 %		
ta-C ref p3	5	95.3 %	4.4 %	0.3 %		
ta-C+Fe(2%) p1	6	93.6 %	5.7 %	0.2 %	0.5 %	
ta-C+Fe(2%) p2	7	93.8 %	5.7 %	0.0 %	0.4 %	
ta-C+Fe(2%) p3	8	93.8 %	5.6 %	0.2 %	0.4 %	
ta-C+Fe(5%) p1	9	90.8 %	7.4 %	0.5 %	1.2 %	
ta-C+Fe(5%) p2	10	90.9 %	7.5 %	0.3 %	1.2 %	
ta-C+Fe(5%) p3	11	91.1 %	7.7 %	0.1 %	1.2 %	
ta-C+Fe(10%) p1	12	85.6 %	11.1 %	0.8 %	2.5 %	
ta-C+Fe(10%) p2	13	86.8 %	10.6 %	0.2 %	2.5 %	
ta-C+Fe(10%) p3	14	86.9 %	10.2 %	0.6 %	2.4 %	
Aalto XPS ref		**C 1s**	**O 1s**			
what	0	59.1 %	40.9 %			
what	2	60.2 %	39.8 %			

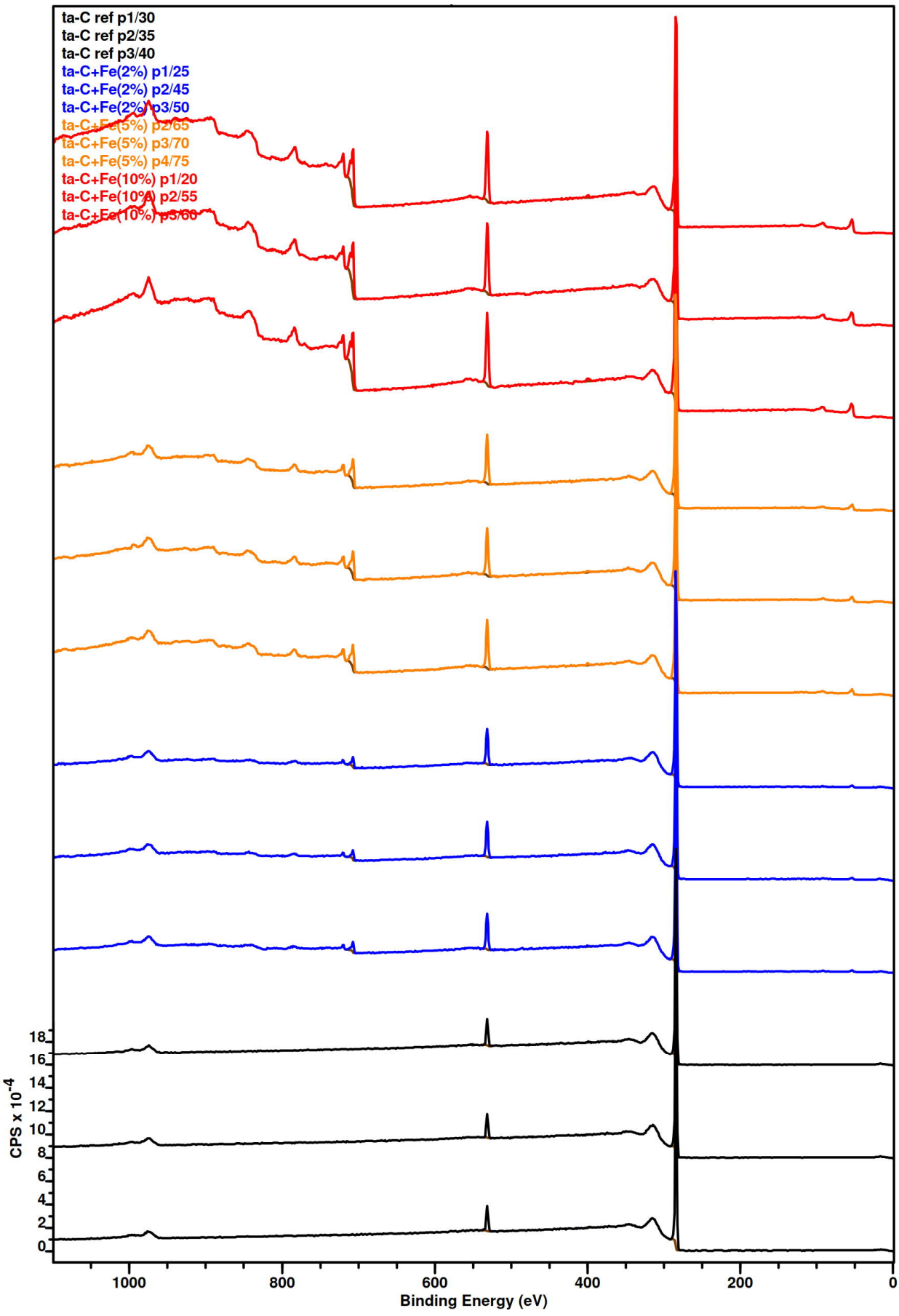

Figure S3. Individual X-ray photoelectron spectroscopy (XPS) survey spectra of investigated samples.

Supplementary C: Transmission electron microscopy

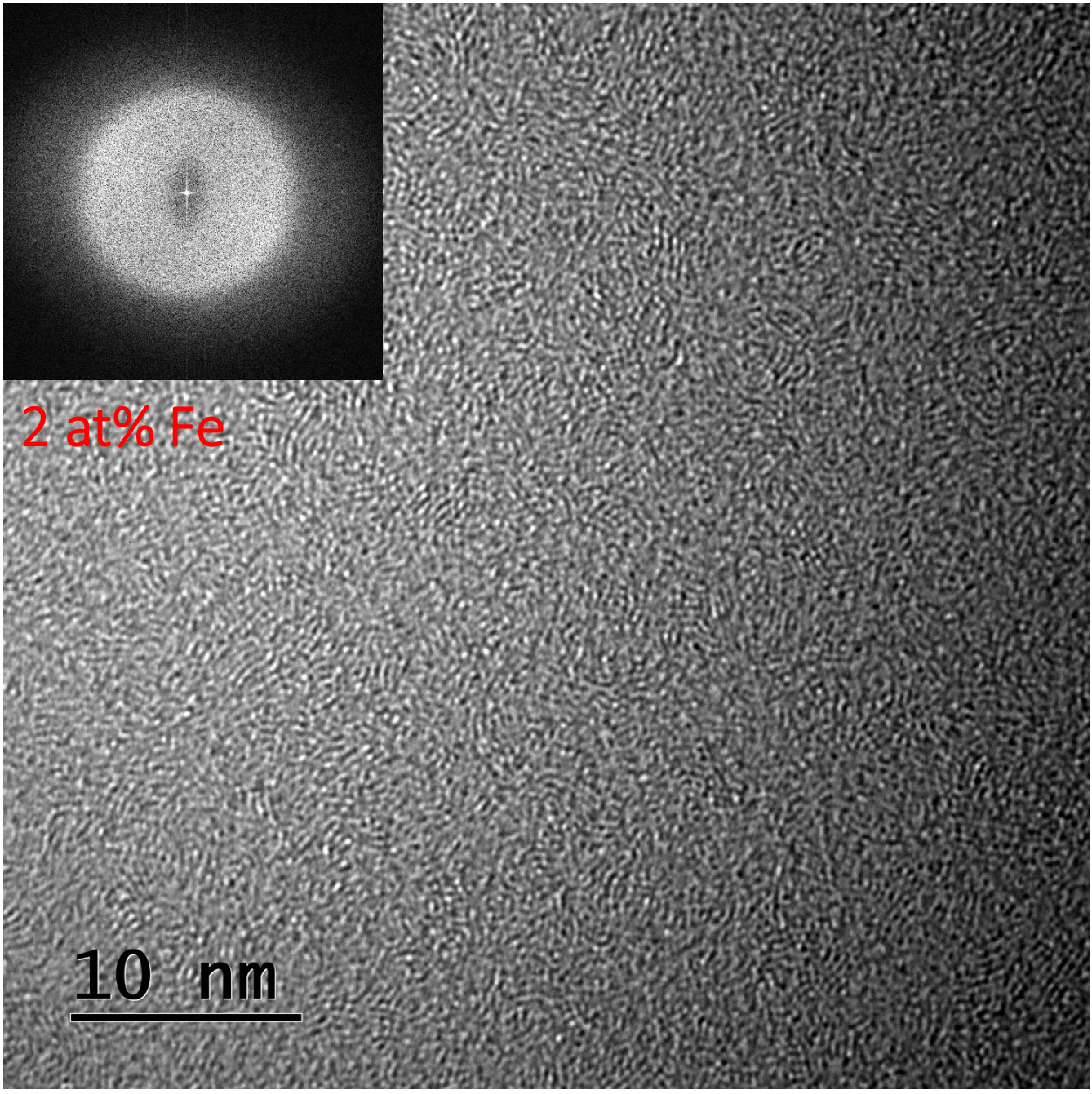

Figure S4. Planar 440kx TEM micrograph of 2 at% Fe sample from a typical area showing no particle growth in the matrix. Inset shows a fast Fourier transform of the image.

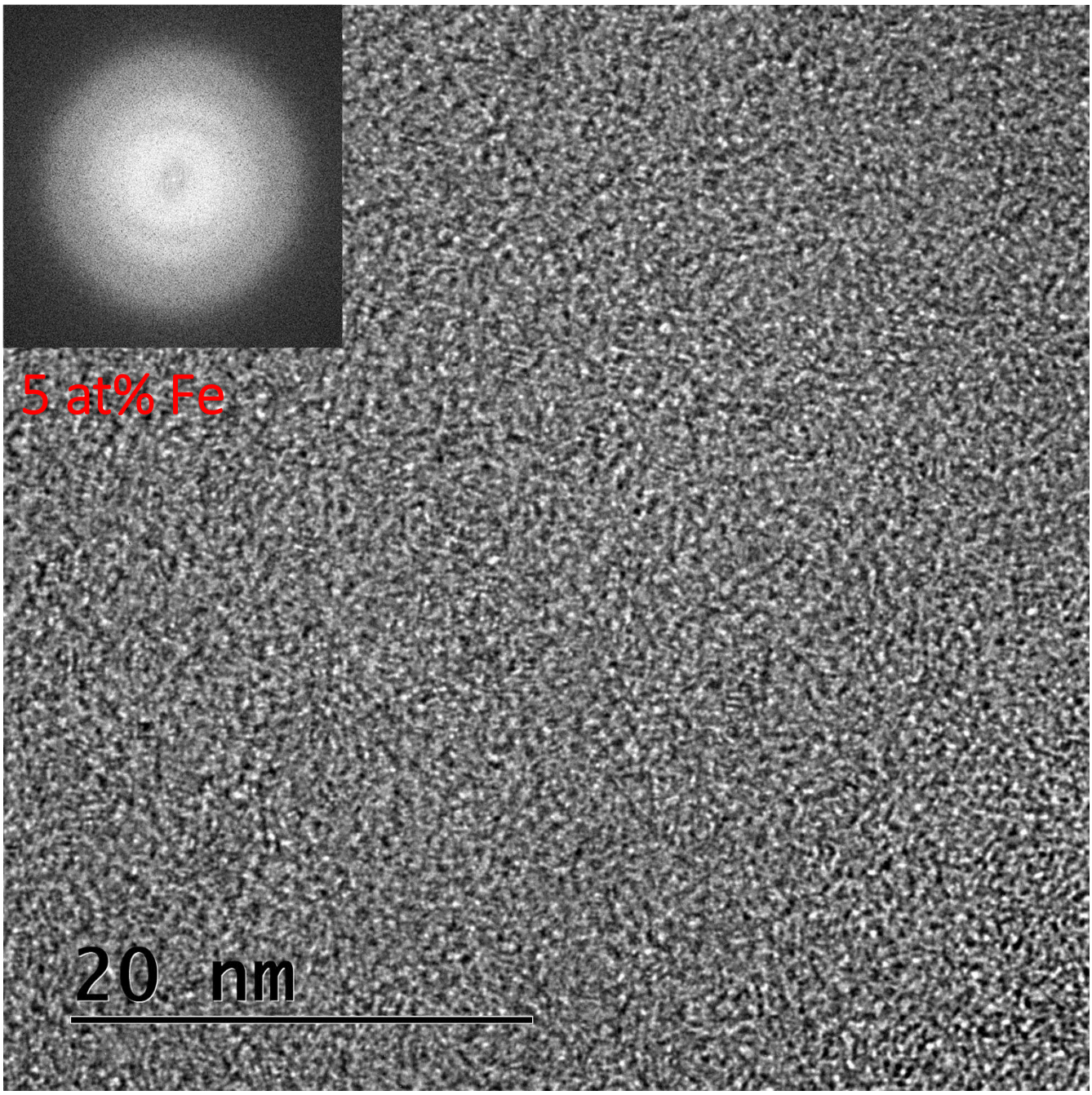

Figure S5. Planar 440kx TEM micrograph of 5 at% Fe sample from a typical area showing no particle growth in the matrix. Inset shows a fast Fourier transform of the image.

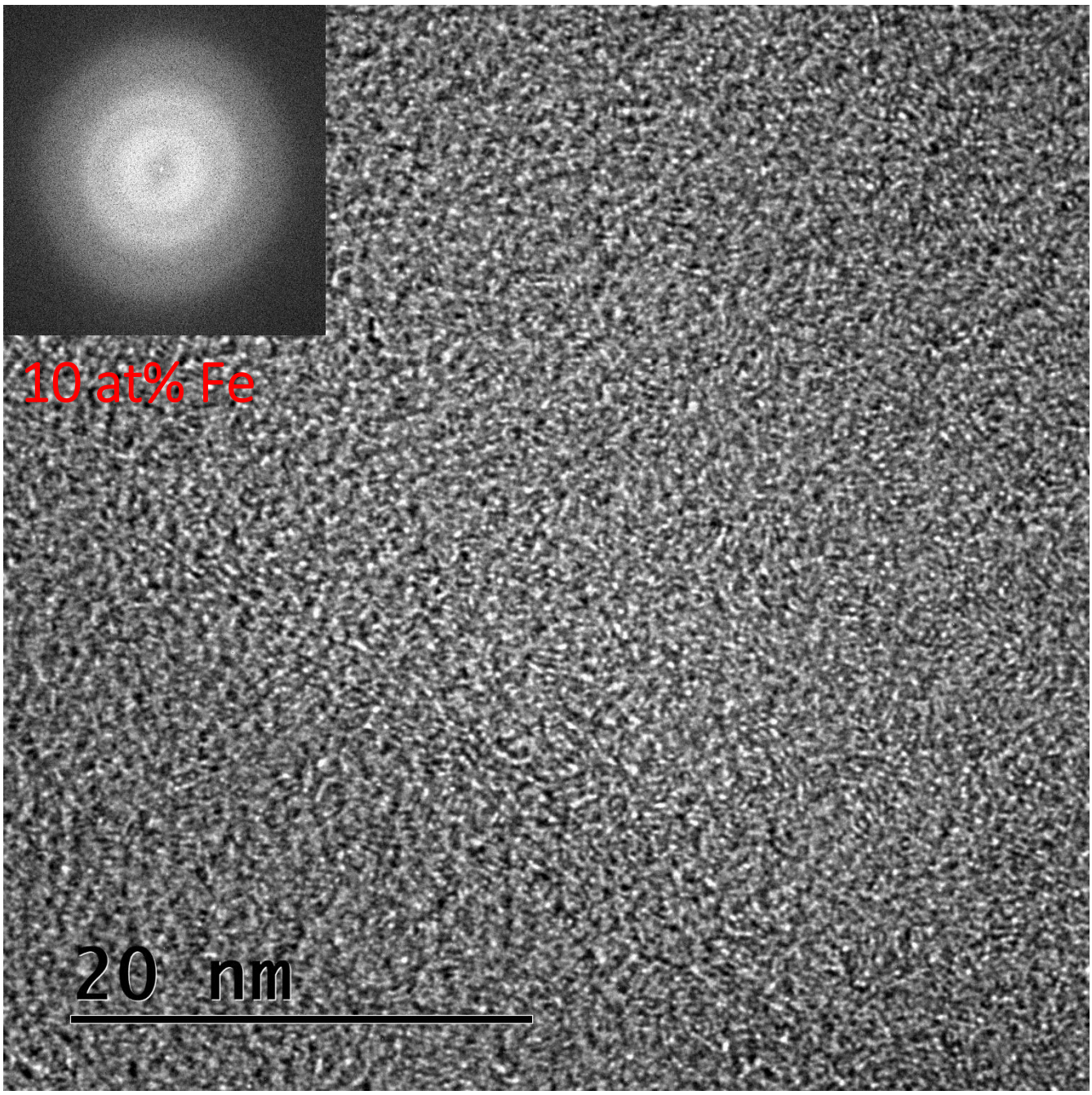

Figure S6. Planar 440kx TEM micrograph of 10 at% Fe sample from a typical area showing no particle growth in the matrix. Inset shows a fast Fourier transform of the image.

Supplementary D: Electrochemistry

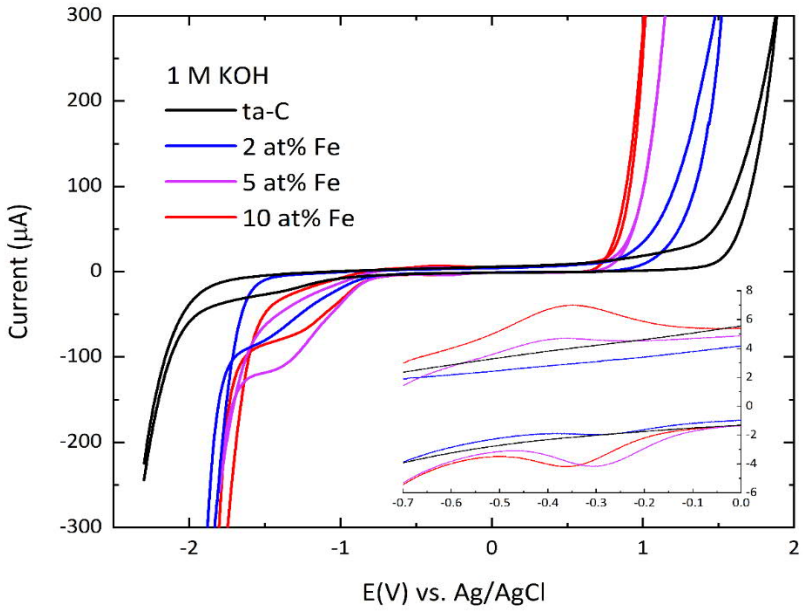

Figure S7. Cyclic voltammogram of 1 M KOH in 400 mV/s for a 200 μA threshold. The inset shows a redox couple attributable to iron species.

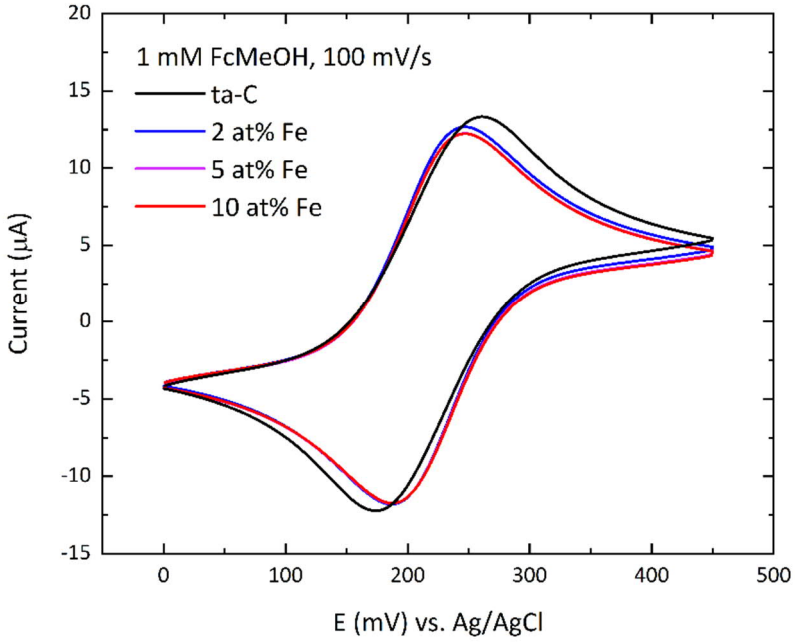

Figure S8. Cyclic voltammogram of 1 mM FcMeOH in 1 M KCl in 100 mV/s scan speed.

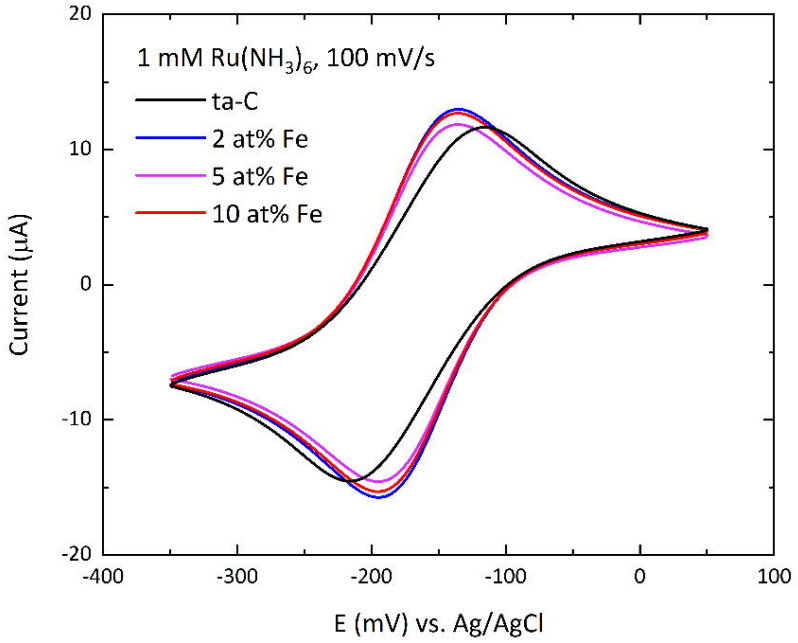

Figure S9. Cyclic voltammogram of 1 mM $Ru(NH_3)_6$ in 1 M KCl in 100 mV/s scan speed.

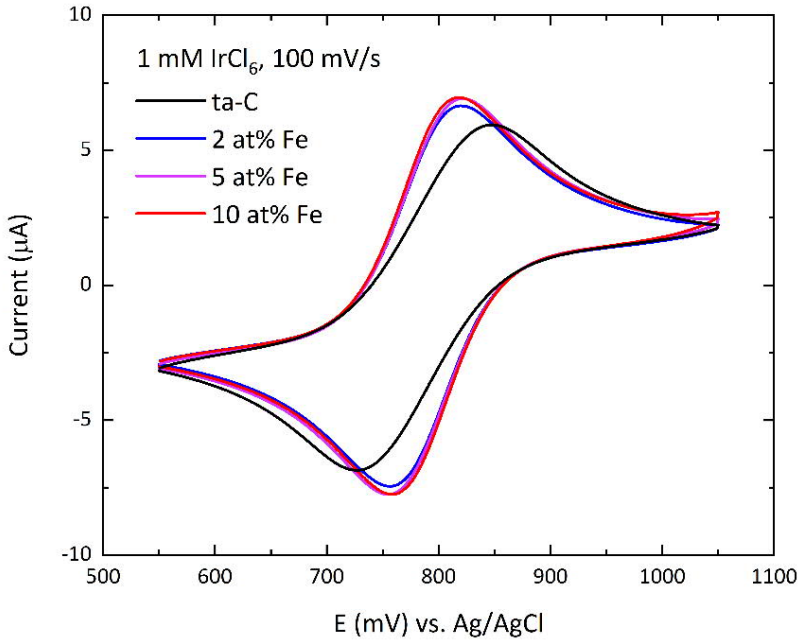

Figure S10. Cyclic voltammogram of 1 mM $IrCl_6$ in 1 M KCl in 100 mV/s scan speed.

Linear correlation of redox peak currents (I_p) as a function of square root of scan speed ($v^{(1/2)}$) indicate the outer sphere redox probe reactions are diffusion controlled (Fig S11-S13).

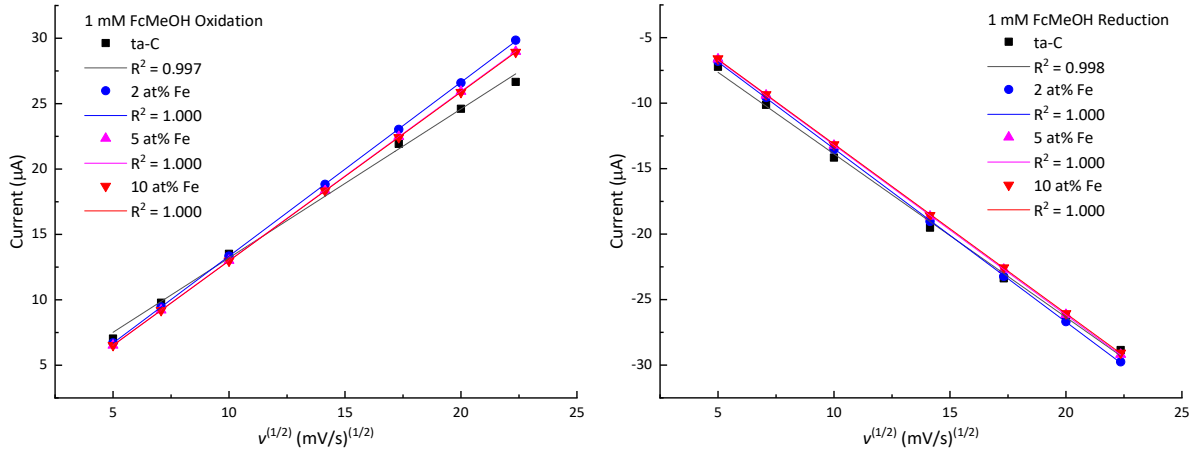

Figure S11. Linear correlation of redox peak currents (I_p) for oxidation (left) and reduction (right) as a function of $v^{(1/2)}$ in 1 mM FcMeOH in 1 M KCl.

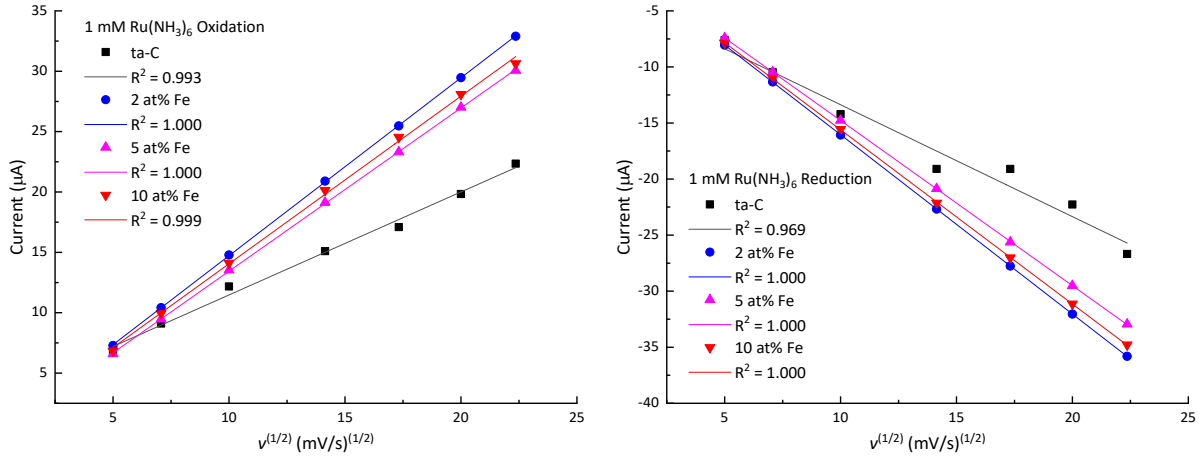

Figure S12. Linear correlation of redox peak currents (I_p) for oxidation (left) and reduction (right) as a function of $v^{(1/2)}$ in 1 mM $Ru(NH_3)_6$ in 1 M KCl.

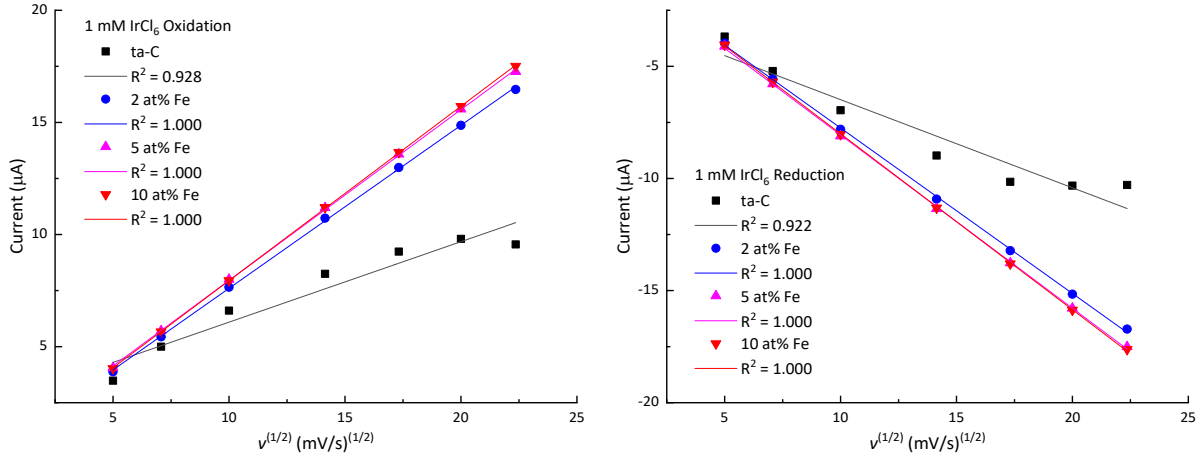

Figure S13. Linear correlation of redox peak currents (I_p) for oxidation (left) and reduction (right) as a function of $v^{(1/2)}$ in 1 mM $IrCl_6$ in 1 M KCl.

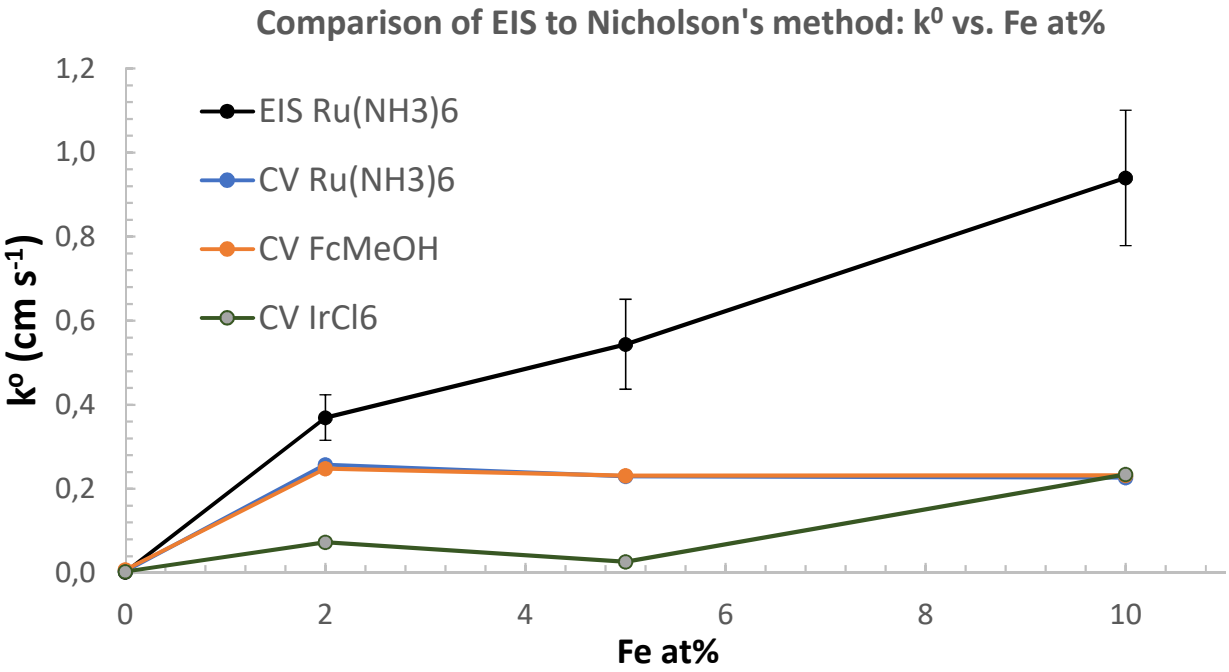

Figure S14. Comparison of rate constants (k^0) calculated from CV data (Nicholson's method) and EIS (N=3). Rate constants calculated from CV data for the three redox probes are the averages of all measured scan speeds.